Role of Bile Acid Pathway Intermediates in Pathology of CTX

William J. Griffiths, Eylan Yutuc, Mohsen Ali Asgari and Yuqin Wang

Swansea University Medical School, ILS1 Building, Singleton Park, Swansea SA2 8PP, Wales, UK

Abstract

A deficiency in the enzyme sterol 27-hydroxylase (CYP27A1) leads to the autosomal recessive disorder cerebrotendinous xanthomatosis (CTX). CYP27A1 catalyses the first steps of the acidic pathway of bile acid biosynthesis. Most cells express CYP27A1, and a deficiency in this enzyme results in the activation of shunt pathways to help remove excess cholesterol. CYP27A1 also appears in the middle of the neutral pathway of bile acid biosynthesis and its deficiency results in accumulation of up-stream pathway intermediates. Here we describe methods for the simultaneous analysis of almost all metabolites from cholesterol to bile acids in a single assay and discuss the relative importance of accumulation of pathway intermediates and missing metabolites to the pathology of CTX.

Introduction

The identification of sterol 27-hydroxylase (cytochrome P450 family 27 subfamily A member 1, CYP27A1, OMIM 606530) as the deficient enzyme in the autosomal recessive disorder cerebrotendinous xanthomatosis (CTX) was made thanks to the pioneering work of Ingemar Björkhem and David Russell in the 1980's and 1990's (1-3). CYP27A1 represents the first enzyme of the acidic pathway of bile acid synthesis introducing a hydroxy group at the terminal carbon of the sterol side-chain with resultant R stereochemistry at C-25 and further converts this primary alcohol to a carboxylic acid (Figure 1) (4). The enzymatic products 27-hydroxycholesterol (27-HC), systematically but less commonly named (25R)26-hydroxycholesterol (5), and 3β-hydroxycholest-5-en-(25R)26-oic acid (3β-HCA) are then metabolised through multiple steps to primary bile acids, mostly chenodeoxycholic acid (CDCA) (4). Note, stereochemistry at C-25 in C_{27} sterols is assumed to be 25R unless stated otherwise. CYP27A1 also appears in the neutral pathway of bile acid biosynthesis converting 7α,12α-dihydroxycholesterol (7α,12α-diHC), 7α,12α-dihydroxycholest-4-en-3-one (7α,12α-diHCO) and their reduced metabolite 5β-cholestan-3α,7α,12α-triol to their respective C_{27} carboxylic acids ready for side-chain shortening to ultimately give cholic acid (Figure 1). The pathology of CTX is often explained by a build up of toxic intermediates up-stream of CYP27A1 in the neutral pathway and many of the clinical features of CTX can be resolved by treatment with CDCA (6). However, CDCA does not appear to be effective in treating some of the neurological aspects of CTX and alternative strategies to restore the functional enzyme may have merit.

Figure 1. Abbreviated versions of the acidic and neutral pathways of bile acid biosynthesis. Metabolites absent or greatly diminished in plasma from CTX patients are indicated by a downward pointing thick red arrow, those elevated by an upward pointing thick blue arrow. The enzyme CYP27A1 is shown in red, other enzymes in blue. Defective reactions in CTX are shown by a crossed arrow. Cholesterol is drawn in red, its metabolites detected by positive-ion LC-ESI-MS^n following treatment with cholesterol oxidase and [$^2H_5$]GP (Fr-1A) are in green, those detected following [$^2H_0$]GP derivatisation in the absence of cholesterol oxidase treatment (Fr-1B) are in claret, and those with a 5α-hydroxy plus carboxylic acid group detected by negative-ion LC-ESI-MS^n are shown in brown. A cholestanetetrol GlcA is shown in the inset with the GlcA arbitrarily drawn attached to C-25.

CTX is an autosomal recessive disorder, and in cases where a pathological mutation is present in both alleles of CYP27A1 with the result of a largely inactive enzyme, diagnosis can be made by gene sequencing, assuming the mutation is known, or by mass spectrometry (MS). This can be by gas-

chromatography (GC)-MS monitoring an elevation in cholestanol (5α-cholestane-3β-ol) in plasma or by monitoring an increase in urinary or plasma bile alcohol glucuronides (GlcA) e.g. cholestanetetrol-, cholestanepentol-, cholestanehexol-GlcA, accompanied by a fall in CDCA by direct infusion (DI)-MS or liquid chromatography (LC)-MS (7-10). A disadvantage of cholestanol as a diagnostic of CTX is that it can be elevated in other disorders like familial hypercholesterolemia and sitosterolaemia (10). Diagnosis may be more difficult in cases where some enzyme activity is maintained, in which case it may be prudent to monitor additional metabolites like 27-HC and 3β-HCA which will be almost absent when the enzyme is inactive but present at a reduced concentration where partial activity is maintained, or 7α-hydroxycholest-4-en-3-one (7α-HCO) and 7αH,12α-diHCO which are elevated when CYP27A1 activity is deficient (11).

Measuring Cholesterol Metabolites Characteristic of CTX

GC-MS is applicable for measurement of cholestanol, 7α-hydroxycholesterol (7α-HC) and 7α-HCO, all of which are elevated in CTX plasma, and Lütjohann et al have recommended the latter two compounds as optimal markers in plasma for monitoring the response to therapy and their ratio to 27-HC, also measured in the same GC-MS run, as a good CTX diagnostic (10). While GC-MS is routinely used in dedicated mass spectrometry laboratories the additional requirement of derivatisation has over the decades led to a shift to more direct analysis methods. Historically elevated levels of bile alcohol glucuronides in urine or plasma/serum have been used to diagnose CTX, first by fast atom bombardment (FAB)-MS and later by electrospray ionisation (ESI)-MS (7-9). Here there is no requirement for derivatisation, just a simple sample clean up, often by solid-phase extraction (SPE). Currently there is a move towards the use of ESI-tandem-MS (MS/MS or MS^2) in the screening for CTX from dried blood spots. Vaz et al have generated convincing data using ESI-MS/MS to demonstrate the ratio of cholestanetetrol-GlcA to taurochenodeoxycholic acid (TCDCA) as a diagnostic for CTX, where cholestanetetrol-GlcA is elevated and TCDCA diminished (12). By also measuring the ratio of taurotrihydroxycholestanoic acid to cholestanetetrol-GlcA confusion with peroxisomal disorders can be avoided where cholestanetetrol-GlcA and taurotrihydroxycholestanoic acid are both elevated, but taurotrihydroxycholestanoic acid will be greatly diminished in CTX. Hong et al have added LC separation to the ESI-MS/MS diagnostic method, concluding that both cholestanetetrol-GlcA and the ratio of cholestanetetrol-GlcA to TCDCA are excellent CTX biomarkers suitable for newborn screening (13).

Measuring Multiple Bile Acid Precursors Elevated in CTX in a Single Analysis

The deficiency in CYP27A1 shifts cholesterol metabolism from the acidic to the neutral pathway, this is accentuated by a lack in production of CDCA resulting in reduced negative feedback via the farnesoid X receptor (FXR) on CYP7A1 expression, the first enzyme of the neutral pathway of bile acid biosynthesis (Figure 1), driving enhanced production of 7α-HC (8). Additionally, the block in the neutral pathway by a defective CYP27A1 results in an elevation in plasma of the early metabolites of the pathway i.e., 7α-HC, 7α-HCO, 7α,12α-diHC and 7α,12α-diHCO. These four metabolites fall into the family of molecules called oxysterols i.e. oxidised forms of cholesterol, which also include 27-HC, 7α,27-dihydroxycholesterol (7α,27-diHC), 7α,27-dihydroxycholest-4-en-3-one (7α,27-diHCO) and the cholestenoic acids all of which are diminished in CTX (14-16). While these molecules can be monitored by GC-MS it requires multiple different derivatisation steps, often with and without additional saponification necessary to hydrolyse sterol esters (17).

To maximise the monitoring of these bile acid precursors we have developed a simple derivatisation strategy which allows the detection of most of the bile acid precursors in a single LC-ESI-$(MS)^n$ experiment (Figure 1) (18). In brief, oxysterols including cholestenoic acids, are extracted from e.g.

plasma, into ethanol and after dilution with water passed through a C_{18} SPE column. Cholesterol and other highly lipophilic components are retained by the column leaving an eluent rich in oxysterols including cholestenoic acids. This eluate is divided into two equal fractions, Fr-1A and Fr1-B. Both fractions are dried down then reconstituted in propan-2-ol. To Fr-1A bacterial cholesterol oxidase enzyme in phosphate buffer is added. This converts sterols with a 3β-hydroxy group to equivalents 3-ones via the classical Richmond reaction (Figure 2A) (19, 20). [$^2H_5$]Girard P ([$^2H_5$]GP) reagent is then added in methanol, this reacts with the 3-oxo group to give a GP-hydrazone. The reaction mixture can be cleaned-up on a second reversed-phase SPE column to remove excess derivatisation reagent or injected directly onto a trap column preceding the LC column linked to the MS. The derivatised sterols give greatly improved ESI response and intense fragment ions useful for both quantification and identification (Figure 2) (14, 18, 21). However, some oxysterols and cholestenoic acids e.g. 7α-HCO, 7α,12α-diHCO, 7α-hydroxy-3-oxocholest-4-en-(25R/S)26-oic acid (7αH,3O-CA), naturally possess a native 3-oxo group and do not require an oxidation step prior to derivatisation. These can be analysed directly from Fr-1B which is treated as Fr-1A but in the absence of cholesterol oxidase and with the use of [$^2H_0$]GP instead of [$^2H_5$]GP (Figure 2B). The use of different isotopic GP reagents means that after the second SPE step equal aliquots of Fr-1A and Fr-1B can be combined and analysed in combination by LC-ESI-MS^n providing complementary information on cholesterol metabolites. Sterols derivatised with [$^2H_5$]GP can be differentiated from those derivatised with [$^2H_0$]GP by virtue of their difference in mass (5.0314 Da). This protocol allows the identification of all major cholesterol metabolites in the bile acid biosynthesis pathway with a 3β-hydroxy or 3-oxo group (Figure 1) and with the inclusion of internal standards absolute quantification (18).

Figure 2. Measuring multiple bile acid precursors via simple derivatisation and LC-ESI-MS^n. (A) Cholesterol metabolites with a 3β-hydroxy-5-ene structure are converted by bacterial cholesterol oxidase in the Richmond reaction to the equivalent 3-oxo-4-enes which are then derivatised with [$^2H_5$]GP (i.e. Fr-1A). (B) Metabolites with a native 3-oxo group are derivatised directly with [$^2H_0$]GP (i.e. Fr-1B). Fr-1A and Fr-1B are combined and analysed by LC-ESI-MS^n. Note, positive-negative ion switching allows the detection of bile acid precursor with a 3α-hydroxy group which are transparent to this derivatisation, providing they also have a carboxylic acid group. (C) Derivatised metabolites fragment by MS^2 to give abundant fragment-ions valuable for multiple-reaction monitoring and by MS^3 to give structural information.

From data generated using this methodology the best CTX diagnostics in plasma are revealed to be concentration ratios of 7α,12α-diHCO to 27-HC, 7α,12α-diHCO to 3β-HCA and 7α,12α-diHCO to 7αH,3O-CA (Figure 3) (14-16, 22). In each case there is no overlap in the measured ratios between control and CTX plasma and for the latter two ratios the controls differ from CTX by about three orders of magnitude. An advantage of the 7α,12α-diHCO to 7αH,3O-CA ratio is that both metabolites can be analysed in Fr-1B i.e. Fr-1A does not require preparation or analysis.

Figure 3. Ratios of bile acid precursors in plasma give unequivocal diagnosis of CTX. Ratios are shown on a log scale. Data from control samples are shown in blue (n = 24), from CTX patients on bile acid therapy are shown in red (n = 14), from untreated CTX patients in green (n = 4), and from CTX patients where treatment is unknown in purple (n = 4). In the case of 7αH,3O-CA measurements were made from 12 CTX patients on bile acid therapy, 3 patients not on treatment, and one patient where the treatment regime was not known. Data from Griffiths et al 2013 (14), Theofilopoulos et al 2014 (15), Abdel-Khalik et al 2017 (22) and Hoflinger et al 2021 (16).

Unexpected Bile Acid Precursors in Plasma and CSF

CYP27A1 introduces the 27-hydroxy and 27-carboxy groups onto the side-chain of cholesterol and other sterols leading to R-stereochemistry at the asymmetric centre at C-25. Other CYP enzymes can also hydroxylate the terminal carbon of sterols including CYP46A1 and CYP3A (23, 24) and we have found that CYP3A4 will 27-hydoxylate 7α-HC to 7α,27-diHC to specifically give S-stereochemistry at C-25, i.e. 7α,27-diHC(25S) (25).

When plasma or CSF is analysed from control individuals the cholestenoic acid 7αH,3O-CA is observed as both the 25R and 25S isomers, the latter being about 10 – 20% of the abundance of the former, with the two isomers being interconvertible through via CoA-thioesters by the enzyme alpha-methylacyl-CoA-racemase (AMACR) (4, 18). Interesting, in CTX we also find both isomers at very low levels but of quite similar abundance (16, 18). This leads to the hypothesis that in CTX elevated 7α-HC can be hydroxylated by CYP3A4 to 7α,27-diHC(25S) which can the undergo oxidation by 3β-hydroxy-Δ^5-steroid oxidoreductase (HSD3B7) and further oxidation, perhaps by CYP3A4 or another oxygenase, at the terminal carbon to give 7αH,3O-CA(25S). This acid can undergo side-chain shortening and may account for the presence of low levels of CDCA sometimes observed in CTX. Alternatively, 7αH,3O-CA(25S) can isomerise to 7αH,3O-CA(25R) (4).

Bile Acid Precursors in Human Brain

In human brain the major cholesterol metabolite is 24S-hydroxycholesterol (24S-HC), this can be exported from brain and transported in the circulation to the liver for conversion to bile acids (26). Unlike cholesterol, oxysterols can cross the blood brain barrier, in this way 24S-HC is exported from while 27-HC imported into brain. We have analysed a single brain sample from a CTX patient (16). Levels of 24S-HC were similar to controls, but 27-HC was absent in CTX while 7α-HCO and 7α,12α-diHCO were both elevated in CTX, as was cholestanol (16). Presumably both 7α-HCO and 7α,12α-diHCO enter the brain from the circulation as the necessary 7α- and 12α-hydroxylases (CYP7A1 and CYP8B1) are not expressed in brain (27). Interestingly, 7α,12α-diHCO and cholestanol were not found to be toxic to a neuronal-like cell line suggesting that some of the neurological problems associated with CTX may not be a consequence of toxic metabolites but rather an absence of neuroprotective metabolites (16, 28).

Positive-Negative ion Switching Further Enhances the Confidence of CTX Diagnosis by MS

As discussed above LC-ESI-MS^n following GP-derivatisation allows the detection of all abundant bile acid precursors with a 3β-hydroxy or 3-oxo functional group. This is performed in the positive-ion MS mode. However, primary bile acids and their immediate precursors possess a 3α-hydroxy group and are transparent to cholesterol oxidase treatment and GP-derivatisation. However, these metabolites often possess a carboxy group or are conjugated with GlcA and can be readily analysed in the negative-ion MS mode. So if we follow the cholesterol oxidase and GP-derivatisation protocol with positive-negative ion switching we can detect bile acid pathway intermediates with a 3β-hydroxy, 3-oxo or 3α-hydroxy group providing the latter have also a carboxy group. This covers almost the entire bile acid biosynthesis pathway plus a shunt to the bile alcohol glucuronides and cholestanol (Figure 1).

Conclusions

While genome sequencing can identify mutations in CYP27A1, to translate this data definitively into enzyme activity requires the measurement of enzymatic products. This can be performed with comparative ease by current MS methods providing a definitive diagnosis. This is likely to become evermore important with the uncovering of variants of unknown significance and in cases of late onset CTX. In addition, the best way to determine a deficiency in CYP27A1 activity in the realm of newborn screening is by MS.

Acknowledgements

This work was supported by funding from the UKRI (BBSRC grant numbers BB/l001735/1, BB/S019588/1, MR/X012387/1 and MR/Y008057/1 to WJG, BB/L001942/1 to YW), and the European Union, through European Structural Funds (ESF), as part of the Welsh Government funded Academic Expertise for Business project (to WJG and YW). For the purpose of open access, the authors have applied a CC BY public copyright license to any Author Accepted Manuscript version arising.

Declaration of competing interests

The authors declare the following financial interests/personal relationships which may be considered as potential competing interests: WJG and YW are listed as inventors on the patent "Kit and method for quantitative detection of steroids" US9851368B2 and the patent application "Compound and method for the treatment and diagnosis of neurodegenerative conditions" US 2021/0139529 A1. WJG, EY and YW are shareholders in CholesteniX Ltd.

References

1. Skrede, S., I. Björkhem, E. A. Kvittingen, M. S. Buchmann, S. O. Lie, C. East, and S. Grundy. 1986. Demonstration of 26-hydroxylation of C27-steroids in human skin fibroblasts, and a deficiency of this activity in cerebrotendinous xanthomatosis. *J Clin Invest* **78**: 729-735.
2. Cali, J. J., C. L. Hsieh, U. Francke, and D. W. Russell. 1991. Mutations in the bile acid biosynthetic enzyme sterol 27-hydroxylase underlie cerebrotendinous xanthomatosis. *J Biol Chem* **266**: 7779-7783.
3. Bjorkhem, I. 2013. Cerebrotendinous xanthomatosis. *Curr Opin Lipidol* **24**: 283-287.
4. Russell, D. W. 2003. The enzymes, regulation, and genetics of bile acid synthesis. *Annu Rev Biochem* **72**: 137-174.
5. Fakheri, R. J., and N. B. Javitt. 2012. 27-Hydroxycholesterol, does it exist? On the nomenclature and stereochemistry of 26-hydroxylated sterols. *Steroids* **77**: 575-577.
6. Berginer, V. M., G. Salen, and S. Shefer. 1984. Long-term treatment of cerebrotendinous xanthomatosis with chenodeoxycholic acid. *N Engl J Med* **311**: 1649-1652.
7. Egestad, B., P. Pettersson, S. Skrede, and J. Sjövall. 1985. Fast atom bombardment mass spectrometry in the diagnosis of cerebrotendinous xanthomatosis. *Scand J Clin Lab Invest* **45**: 443-446.
8. Clayton, P. T. 2011. Disorders of bile acid synthesis. *J Inherit Metab Dis* **34**: 593-604.
9. Setchell, K. D., and J. E. Heubi. 2006. Defects in bile acid biosynthesis--diagnosis and treatment. *J Pediatr Gastroenterol Nutr* **43 Suppl 1**: S17-22.
10. Lütjohann, D., F. Stellaard, and I. Björkhem. 2020. Levels of 7alpha-hydroxycholesterol and/or 7alpha-hydroxy-4-cholest-3-one are the optimal biochemical markers for the evaluation of treatment of cerebrotendinous xanthomatosis. *J Neurol* **267**: 572-573.
11. DeBarber, A. E., Y. Sandlers, A. S. Pappu, L. S. Merkens, P. B. Duell, S. R. Lear, S. K. Erickson, and R. D. Steiner. 2011. Profiling sterols in cerebrotendinous xanthomatosis: utility of Girard derivatization and high resolution exact mass LC-ESI-MS(n) analysis. *J Chromatogr B Analyt Technol Biomed Life Sci* **879**: 1384-1392.
12. Vaz, F. M., Y. Jamal, R. Barto, M. H. Gelb, A. E. DeBarber, R. A. Wevers, M. R. Nelen, A. Verrips, A. H. Bootsma, M. J. Bouva, N. Kleise, W. van der Zee, T. He, G. S. Salomons, and H. H. Huidekoper. 2023. Newborn screening for Cerebrotendinous Xanthomatosis: A retrospective biomarker study using both flow-injection and UPLC-MS/MS analysis in 20,000 newborns. *Clin Chim Acta* **539**: 170-174.
13. Hong, X., J. Daiker, M. Sadilek, A. E. DeBarber, J. Chiang, J. Duan, A. H. Bootsma, H. H. Huidekoper, F. M. Vaz, and M. H. Gelb. 2020. Toward newborn screening of cerebrotendinous xanthomatosis: results of a biomarker research study using 32,000 newborn dried blood spots. *Genet Med* **22**: 1606-1612.

14. Griffiths, W. J., P. J. Crick, Y. Wang, M. Ogundare, K. Tuschl, A. A. Morris, B. W. Bigger, P. T. Clayton, and Y. Wang. 2013. Analytical strategies for characterization of oxysterol lipidomes: liver X receptor ligands in plasma. *Free Radic Biol Med* **59**: 69-84.
15. Theofilopoulos, S., W. J. Griffiths, P. J. Crick, S. Yang, A. Meljon, M. Ogundare, S. S. Kitambi, A. Lockhart, K. Tuschl, P. T. Clayton, A. A. Morris, A. Martinez, M. A. Reddy, A. Martinuzzi, M. T. Bassi, A. Honda, T. Mizuochi, A. Kimura, H. Nittono, G. De Michele, R. Carbone, C. Criscuolo, J. L. Yau, J. R. Seckl, R. Schule, L. Schols, A. W. Sailer, J. Kuhle, M. J. Fraidakis, J. A. Gustafsson, K. R. Steffensen, I. Bjorkhem, P. Ernfors, J. Sjovall, E. Arenas, and Y. Wang. 2014. Cholestenoic acids regulate motor neuron survival via liver X receptors. *J Clin Invest* **124**: 4829-4842.
16. Hoflinger, P., S. Hauser, E. Yutuc, H. Hengel, L. Griffiths, F. Radelfahr, O. W. Howell, Y. Wang, S. L. Connor, P. B. Duell, A. E. DeBarber, P. Martus, D. Lutjohann, W. J. Griffiths, and L. Schols. 2021. Metabolic profiling in serum, cerebrospinal fluid, and brain of patients with cerebrotendinous xanthomatosis. *J Lipid Res* **62**: 100078.
17. Axelson, M., B. Mork, and J. Sjovall. 1988. Occurrence of 3 beta-hydroxy-5-cholestenoic acid, 3 beta,7 alpha-dihydroxy-5-cholestenoic acid, and 7 alpha-hydroxy-3-oxo-4-cholestenoic acid as normal constituents in human blood. *J Lipid Res* **29**: 629-641.
18. Yutuc, E., A. L. Dickson, M. Pacciarini, L. Griffiths, P. R. S. Baker, L. Connell, A. Öhman, L. Forsgren, M. Trupp, S. Vilarinho, Y. Khalil, P. T. Clayton, S. Sari, B. Dalgic, P. Höflinger, L. Schöls, W. J. Griffiths, and Y. Wang. 2021. Deep mining of oxysterols and cholestenoic acids in human plasma and cerebrospinal fluid: Quantification using isotope dilution mass spectrometry. *Anal Chim Acta* **1154**: 338259.
19. Richmond, W. 1976. Use of cholesterol oxidase for assay of total and free cholesterol in serum by continuous-flow analysis. *Clin Chem* **22**: 1579-1588.
20. MacLachlan, J., A. T. Wotherspoon, R. O. Ansell, and C. J. Brooks. 2000. Cholesterol oxidase: sources, physical properties and analytical applications. *J Steroid Biochem Mol Biol* **72**: 169-195.
21. Karu, K., M. Hornshaw, G. Woffendin, K. Bodin, M. Hamberg, G. Alvelius, J. Sjovall, J. Turton, Y. Wang, and W. J. Griffiths. 2007. Liquid chromatography-mass spectrometry utilizing multi-stage fragmentation for the identification of oxysterols. *J Lipid Res* **48**: 976-987.
22. Abdel-Khalik, J., E. Yutuc, P. J. Crick, J. A. Gustafsson, M. Warner, G. Roman, K. Talbot, E. Gray, W. J. Griffiths, M. R. Turner, and Y. Wang. 2017. Defective cholesterol metabolism in amyotrophic lateral sclerosis. *J Lipid Res* **58**: 267-278.
23. Mast, N., R. Norcross, U. Andersson, M. Shou, K. Nakayama, I. Bjorkhem, and I. A. Pikuleva. 2003. Broad substrate specificity of human cytochrome P450 46A1 which initiates cholesterol degradation in the brain. *Biochemistry* **42**: 14284-14292.
24. Honda, A., G. Salen, Y. Matsuzaki, A. K. Batta, G. Xu, E. Leitersdorf, G. S. Tint, S. K. Erickson, N. Tanaka, and S. Shefer. 2001. Side chain hydroxylations in bile acid biosynthesis catalyzed by CYP3A are markedly up-regulated in Cyp27-/- mice but not in cerebrotendinous xanthomatosis. *J Biol Chem* **276**: 34579-34585.
25. Griffiths, W. J., P. J. Crick, A. Meljon, S. Theofilopoulos, J. Abdel-Khalik, E. Yutuc, J. E. Parker, D. E. Kelly, S. L. Kelly, E. Arenas, and Y. Wang. 2019. Additional pathways of sterol metabolism: Evidence from analysis of Cyp27a1-/- mouse brain and plasma. *Biochim Biophys Acta Mol Cell Biol Lipids* **1864**: 191-211.
26. Bjorkhem, I. 2007. Rediscovery of cerebrosterol. *Lipids* **42**: 5-14.
27. Baloni, P., C. C. Funk, J. Yan, J. T. Yurkovich, A. Kueider-Paisley, K. Nho, A. Heinken, W. Jia, S. Mahmoudiandehkordi, G. Louie, A. J. Saykin, M. Arnold, G. Kastenmüller, W. J. Griffiths, I. Thiele, R. Kaddurah-Daouk, and N. D. Price. 2020. Metabolic Network Analysis Reveals Altered Bile Acid Synthesis and Metabolism in Alzheimer's Disease. *Cell Rep Med* **1**: 100138.
28. Theofilopoulos, S., Y. Wang, S. S. Kitambi, P. Sacchetti, K. M. Sousa, K. Bodin, J. Kirk, C. Salto, M. Gustafsson, E. M. Toledo, K. Karu, J. A. Gustafsson, K. R. Steffensen, P. Ernfors, J. Sjovall, W. J. Griffiths, and E. Arenas. 2013. Brain endogenous liver X receptor ligands selectively promote midbrain neurogenesis. *Nat Chem Biol* **9**: 126-133.

Figure Captions

Figure 1. Abbreviated versions of the acidic and neutral pathways of bile acid biosynthesis. Metabolites absent or greatly diminished in plasma from CTX patients are indicated by a downward pointing thick red arrow, those elevated by an upward pointing thick blue arrow. The enzyme CYP27A1 is shown in red, other enzymes in blue. Defective reactions in CTX are shown by a crossed arrow. Cholesterol is drawn in red, its metabolites detected by positive-ion LC-ESI-MS^n following treatment with cholesterol oxidase and [$^2H_5$]GP (Fr-1A) are in green, those detected following [$^2H_0$]GP derivatisation in the absence of cholesterol oxidase treatment (Fr-1B) are in claret, and those with a 5α-hydroxy plus carboxylic acid group detected by negative-ion LC-ESI-MS^n are shown in brown. A cholestanetetrol GlcA is shown in the inset with the GlcA arbitrarily drawn attached to C-25.

Figure 2. Measuring multiple bile acid precursors via simple derivatisation and LC-ESI-MS^n. (A) Cholesterol metabolites with a 3β-hydroxy-5-ene structure are converted by bacterial cholesterol oxidase in the Richmond reaction to the equivalent 3-oxo-4-enes which are then derivatised with [$^2H_5$]GP (i.e. Fr-1A). (B) Metabolites with a native 3-oxo group are derivatised directly with [$^2H_0$]GP (i.e. Fr-1B). Fr-1A and Fr-1B are combined and analysed by LC-ESI-MS^n. Note, positive-negative ion switching allows the detection of bile acid precursor with a 3α-hydroxy group which are transparent to this derivatisation, providing they also have a carboxylic acid group. (C) Derivatised metabolites fragment by MS^2 to give abundant fragment-ions valuable for multiple-reaction monitoring and by MS^3 to give structural information.

Figure 3. Ratios of bile acid precursors in plasma give unequivocal diagnosis of CTX. Ratios are shown on a log scale. Data from control samples are shown in blue (n = 24), from CTX patients on bile acid therapy are shown in red (n = 14), from untreated CTX patients in green (n = 4), and from CTX patients where treatment is unknown in purple (n = 4). In the case of 7αH,3O-CA measurements were made from 12 CTX patients on bile acid therapy, 3 patients not on treatment, and one patient where the treatment regime was not known.

Figure 1

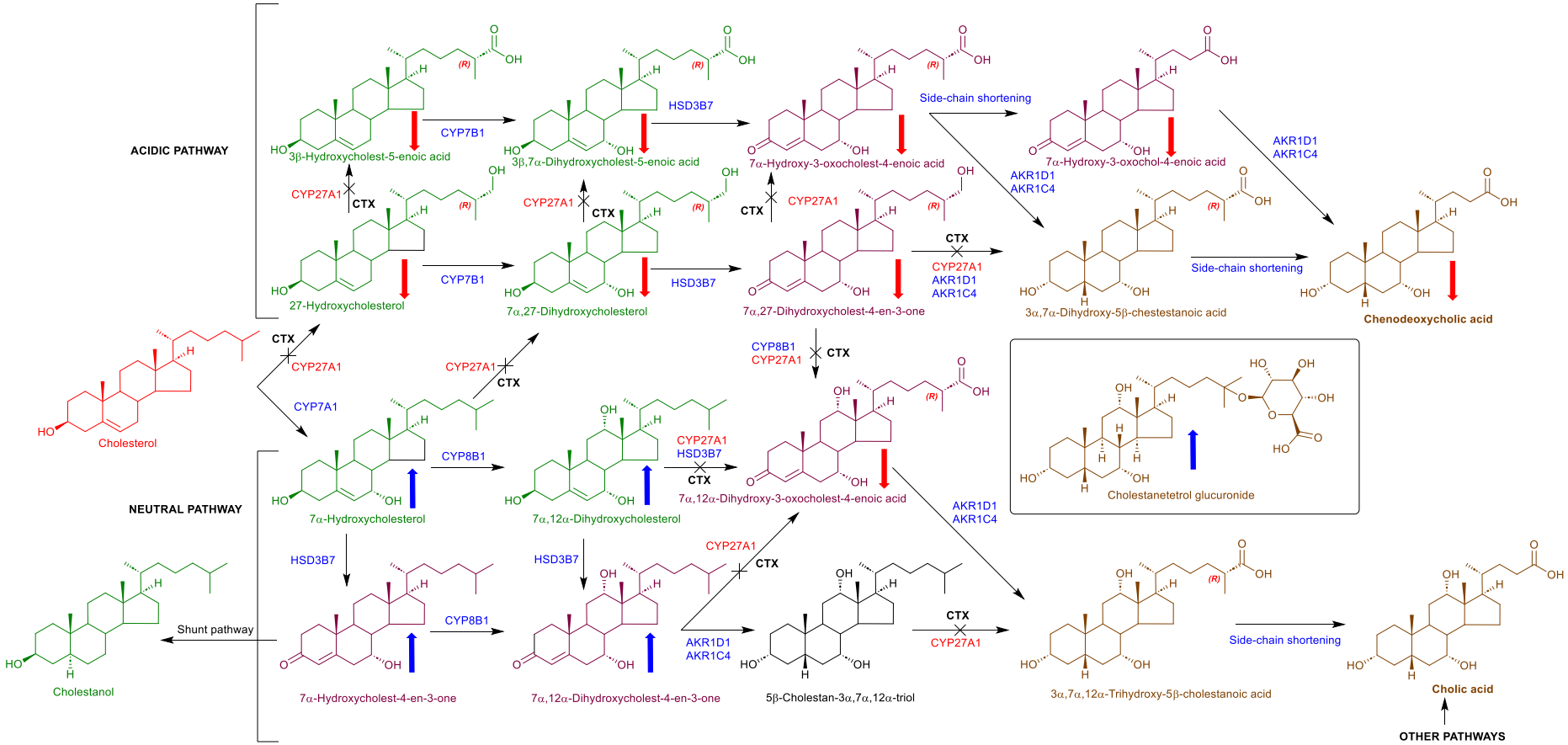
ACIDIC PATHWAY
NEUTRAL PATHWAY
Shunt pathway
Cholesterol
Cholestanol
3β-Hydroxycholest-5-enoic acid
3β,7α-Dihydroxycholest-5-enoic acid
7α-Hydroxy-3-oxocholest-4-enoic acid
7α-Hydroxy-3-oxochol-4-enoic acid
27-Hydroxycholesterol
7α,27-Dihydroxycholesterol
7α,27-Dihydroxycholest-4-en-3-one
3α,7α-Dihydroxy-5β-chestestanoic acid
Chenodeoxycholic acid
7α-Hydroxycholesterol
7α,12α-Dihydroxycholesterol
7α,12α-Dihydroxy-3-oxocholest-4-enoic acid
Cholestanetetrol glucuronide
7α-Hydroxycholest-4-en-3-one
7α,12α-Dihydroxycholest-4-en-3-one
5β-Cholestan-3α,7α,12α-triol
3α,7α,12α-Trihydroxy-5β-cholestanoic acid
Cholic acid
OTHER PATHWAYS
CYP7B1
HSD3B7
CYP27A1
CTX
Side-chain shortening
AKR1D1
AKR1C4
CYP8B1

Figure 2

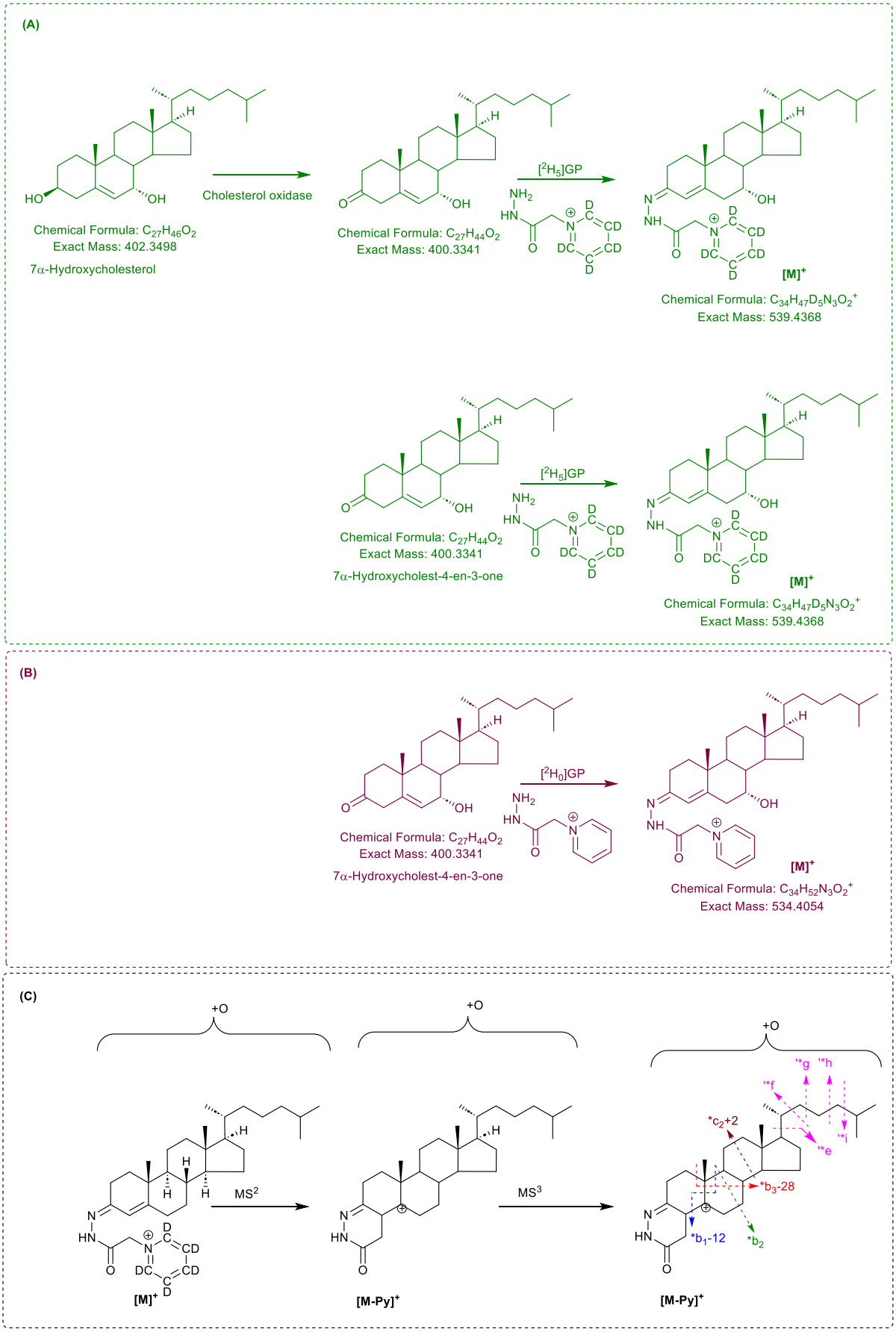
(A)
Cholesterol oxidase
Chemical Formula: C27H46O2
Exact Mass: 402.3498
7α-Hydroxycholesterol
[2H5]GP
Chemical Formula: C27H44O2
Exact Mass: 400.3341
[M]+
Chemical Formula: C34H47D5N3O2+
Exact Mass: 539.4368
[2H5]GP
Chemical Formula: C27H44O2
Exact Mass: 400.3341
7α-Hydroxycholest-4-en-3-one
[M]+
Chemical Formula: C34H47D5N3O2+
Exact Mass: 539.4368
(B)
[2H0]GP
Chemical Formula: C27H44O2
Exact Mass: 400.3341
7α-Hydroxycholest-4-en-3-one
[M]+
Chemical Formula: C34H52N3O2+
Exact Mass: 534.4054
(C)
+O
MS2
MS3
[M]+
[M-Py]+
[M-Py]+
*c2+2
*b3-28
*b1-12
*b2
*e
*f
*g
*h
*i

Figure 3

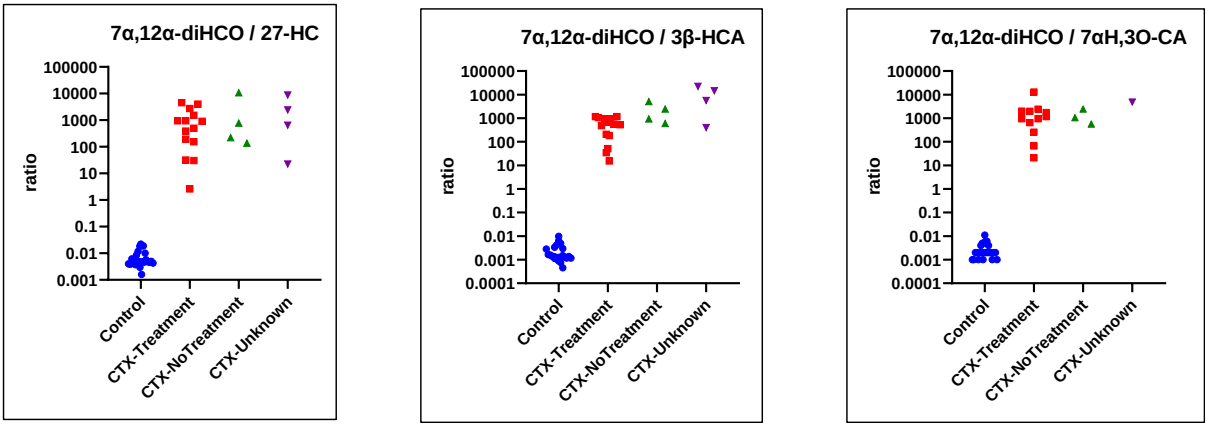
7α,12α-diHCO / 27-HC
ratio
100000
10000
1000
100
10
1
0.1
0.01
0.001
Control
CTX-Treatment
CTX-NoTreatment
CTX-Unknown
7α,12α-diHCO / 3β-HCA
ratio
100000
10000
1000
100
10
1
0.1
0.01
0.001
0.0001
Control
CTX-Treatment
CTX-NoTreatment
CTX-Unknown
7α,12α-diHCO / 7αH,3O-CA
ratio
100000
10000
1000
100
10
1
0.1
0.01
0.001
0.0001
Control
CTX-Treatment
CTX-NoTreatment
CTX-Unknown